Acta Crystallographica Section D
Biological Crystallography
ISSN 0907-4449

Expression, purification, crystallization and preliminary structural characterization of the GTPase domain of human Rheb

Yadong Yu,[a,b] Yonggang Chang,[a,b] Sheng Li,[a,b] Hongyu Hu,[a] Qiuhua Huang[c] and Jianping Ding[a]*

[a]Key Laboratory of Proteomics, Institute of Biochemistry and Cell Biology, Shanghai Institutes for Biological Sciences, Chinese Academy of Sciences, 320 Yue-Yang Road, Shanghai 200031, People's Republic of China, [b]Graduate School of the Chinese Academy of Sciences, People's Republic of China, and [c]State Key Laboratory for Medical Genomics, Shanghai Institute of Hematology, Rui Jin Hospital, Shanghai Second Medical University, 197 Rui-Jin Road II, Shanghai 200025, People's Republic of China

Correspondence e-mail: jpding@sibs.ac.cn

Received 3 July 2004
Accepted 24 July 2004

Ras homologue enriched in brain (Rheb) represents a unique group of small GTPases and shares moderate sequence identity with the Ras/Rap subfamily. It acts downstream of nutrient signalling as the direct target of the tuberous sclerosis complex (TSC) and upstream of mTOR/S6K1/4EBP in the insulin-signalling pathway. The GTPase domain of human Rheb (hRheb) has been recombinantly expressed in *Escherichia coli*, purified and cocrystallized in complexes with GDP, GTP and GppNHp using the hanging-drop vapour-diffusion method. Crystals of the hRheb–GDP complex belong to space group $P2_12_12_1$, with unit-cell parameters $a = 44.5$, $b = 52.3$, $c = 70.6$ Å. The hRheb–GppNHp complex crystallized in two crystal forms: one has the same space group and unit-cell parameters as the hRheb–GDP complex and the other belongs to space group $C222_1$, with unit-cell parameters $a = 102.9$, $b = 99.2$, $c = 48.0$ Å. The hRheb–GTP complex also crystallized in two crystal forms: one belongs to space group $C222_1$, with unit-cell parameters $a = 102.4$, $b = 98.3$, $c = 47.9$ Å, and the other belongs to space group $P2_1$, with unit-cell parameters $a = 77.3$, $b = 47.9$, $c = 71.9$ Å, $\beta = 89.0^\circ$. All these crystals diffract X-rays to better than 2.8 Å resolution and at least one diffraction data set has been collected for each crystal form using an in-house R-AXIS IV^{++} diffractometer. Structural studies of hRheb in complexes with various substrates may provide insights into the recognition and specificity of substrate and the catalytic mechanism of mammalian Rhebs and shed light on the biological functions of Rhebs in the mTOR signalling pathway.

1. Introduction

Small GTPases play important roles in various biological processes including transmembrane signalling, intracellular signal transduction, vesicle trafficking, cytoskeletal rearrangement and neucleoplasmic transport (Herrmann, 2003). They act as binary switches cycling between the active GTP-binding form and the inactive GDP-binding form. GTPase-activating proteins (GAPs) regulate small GTPases by accelerating their low intrinsic GTP hydrolysis activity, while guanosine nucleotide-exchange factors (GEFs) activate them by GDP–GTP exchange. Small GTPases can be divided into six subfamilies: Ras/Rap, Rho, Ran, Rab, Arf and Kir/Rem/Rad (Reuther & Der, 2000). The Ras/Rap subfamily consists of five groups, including the prototypic p21 Ras protein group, which comprises H-Ras, N-Ras and K-Ras. Members of the other groups share about 40–50% amino-acid identity with p21 Ras (Reuther & Der, 2000).

Ras homologue enriched in brain (Rheb) is a small GTPase that was first identified in a differential screen of neuronal genes and subsequently found to be ubiquitously expressed and particularly abundant in muscle and brain (Clark *et al.*, 1997; Gromov *et al.*, 1995; Mizuki *et al.*, 1996; Yamagata *et al.*, 1994). Until recently, its biological functions were unknown. Genetic, biochemical and cell-biological studies in *Drosophila* and mammals have now shown that Rheb participates in the insulin-signalling pathway downstream of tuberous sclerosis complex (TSC) and upstream of the target of rapamycin (TOR) (Li *et al.*, 2004; Manning & Cantley, 2003; Pan *et al.*, 2004; Saucedo *et al.*, 2003; Stocker *et al.*, 2003; Zhang *et al.*, 2003). TSC is an autosomal dominant disorder that is manifested by the occurrence of different types of benign tumours in a variety of organ systems, including the brain, kidneys, lungs, heart, skin, eyes, pancreas and skeleton (Gomez, 1999). TSC syndrome is caused by mutations in either the *TSC1* gene on chromosome 9q34 or the *TSC2* gene on chromosome 16p13 (Dabora *et al.*, 2001; Maheshwar *et al.*, 1997; Povey *et al.*, 1994). The protein products of *TSC1* and *TSC2* genes, hamartin (TSC1) and tuberin (TSC2),

form a putative tumour-suppressor complex (Montagne *et al.*, 2001; Sparagana & Roach, 2000) that regulates the growth-factor-dependent and nutrient-dependent activation of TOR signalling (Gao *et al.*, 2002; Inoki *et al.*, 2002; Jaeschke *et al.*, 2002; Manning *et al.*, 2002; Tee *et al.*, 2002). This repression process is mediated through the small GTPase Rheb (Li *et al.*, 2004; Pan *et al.*, 2004; Saucedo *et al.*, 2003; Stocker *et al.*, 2003; Zhang *et al.*, 2003). TSC2 possesses a domain at its C-terminus that is homologous to Rap1 GAP and Rheb has been shown to be a direct target of the TSC2 GAP domain (Castro *et al.*, 2003; Garami *et al.*, 2003; Inoki *et al.*, 2003; Tee *et al.*, 2003; Zhang *et al.*, 2003). Mammalian Rheb (mRheb) can activate mammalian TOR (mTOR) kinase, which in turn phosphorylates and activates its downstream targets ribosomal S6 kinase 1 (S6K1) and eIF-4E binding protein 1 (4E-BP1) (Castro *et al.*, 2003; Garami *et al.*, 2003; Inoki *et al.*, 2003; Tee *et al.*, 2003). mTOR belongs to the phosphoinositide kinase-related kinase family (PIKK; Hentges *et al.*, 2001; Keith & Schreiber, 1995) and plays a central role in controlling cell growth in response to growth factor, cell energy and nutrient status (Gingras *et al.*, 2001).

Rheb shares a moderate sequence homology with other small GTPase proteins, especially members of the Ras/Rap subfamily (about 30–40% sequence identity; Yamagata *et al.*, 1994). The human *Rheb* gene was localized to both chromosomes 7q36 and 10q11 (Gromov *et al.*, 1995; Mizuki *et al.*, 1996). The human *Rheb* gene-encoded protein (hRheb) consists of 184 amino-acid residues with a molecular weight of 22 kDa (Swiss-Prot code Q15382). The N-terminal 169 residues of hRheb form the GTPase domain. The C-terminal 15 residues have a flexible structure and contain a conserved carboxyl CAA*X* motif that plays important roles in the farnesylation of hRheb and its association with the membrane (Inoki *et al.*, 2003; Castro *et al.*, 2003). The full-length hRheb shares 40% sequence identity with human Rap2A, 37% with human Rap1A and 32% with human H-Ras. Additionally, it also shares 36% sequence identity with human Rab21 and 32% with human RhoA, both of which are not members of the Ras/Rap subfamily.

Extensive structural studies of Ras proteins have been carried out either in unliganded form or in complexes with various ligands and substrates (for reviews, see Herrmann, 2003; Paduch *et al.*, 2001; Vetter & Wittinghofer, 2001). However, so far no three-dimensional structure has been reported for any Rheb. Structural studies of mammalian Rheb in complexes with various substrates may provide a molecular basis for the recognition and specificity of substrate and the catalytic mechanism of Rheb and shed light on the biological functions of Rheb in the mTOR signalling pathway. Comparison of the structure of Rheb with those of other small GTPases may also provide some insight into the evolutionary relationship between Rheb and other small GTPases. In this communication, we report the expression, purification, crystallization and preliminary structural characterization of the GTPase domain of hRheb.

2. Materials and methods

2.1. Cloning, expression and purification

The cDNA corresponding to the GTPase domain (residues 1–169) of hRheb was obtained from the cDNA library of human CD34+ haematopoietic stem/progenitor cells (Zhang *et al.*, 2000). The gene was cloned into the *Nde*I and *Xho*I restriction sites of the pET-22b(+) expression plasmid (Novagen) and fused with a His tag (LEHHHHHH) at the C-terminus. The plasmid was transformed into and expressed in *Escherichia coli* BL21(DE3) strain (Novagen). *E. coli* cells were grown in LB media supplemented with ampicillin (50 $\mu g\ ml^{-1}$) at 310 K until an OD_{600} of 0.6 was reached. Protein expression was induced by adding isopropyl β-D-thiogalactoside (IPTG) to a final concentration of 0.2 m*M*. Cells were cultured for 4 h after induction, collected by centrifugation at 5000*g* for 15 min and resuspended in buffer *A* (50 m*M* NaH_2PO_4 pH 8.0, 500 m*M* NaCl). The cells were further lysed on ice by sonication and the cell debris was precipitated by centrifugation at 15 000*g* for 20 min.

Purification of the protein was carried out by affinity chromatography using an Ni–NTA agarose column (Qiagen). The lysis supernatant was first loaded onto an Ni–NTA agarose column equilibrated with buffer *A* and the resin was washed with 20 column volumes of buffer *B* (buffer *A* supplemented with 20 m*M* imidazole) to elute non-specific binding proteins. The tightly bound target protein was eluted with buffer *C* (buffer *A* supplemented with 250 m*M* imidazole). The final purification was performed using gel filtration on a Superose 12 column (Amersham Pharmacia) with a volume of 60 ml equilibrated with a gel-filtration buffer (50 m*M* Tris–HCl pH 8.0, 200 m*M* NaCl). The fraction containing the target protein was eluted at 40 ml. A similar result was obtained using gel filtration on a Superdex G-75 column (26 × 600 mm, Amersham Pharmacia) with a volume of about 300 ml. The target protein was eluted at about 190 ml. The peak fractions were collected, concentrated and then stored at 193 K in storage buffer (20 m*M* Tris–HCl pH 8.0, 200 m*M* NaCl, 2 m*M* DTT, 0.02% NaN_3, 5 m*M* $MgCl_2$) supplemented with 50% glycerol for biochemical studies and crystallization experiments. All steps were carried out at 277 K to minimize potential proteolysis of the target protein.

Reducing SDS–PAGE analysis of the purified protein shows a single band at 20 kDa. Dynamic light-scattering analysis was carried out by using a DynaPro MS X instrument (Protein Solutions) and the software *DYNAMICS* 5.0 to characterize the aggregation state of the protein in solution (at a protein concentration of 1 $mg\ ml^{-1}$). The protein had a radius of 2.2 nm at 278 K and 2.1 nm at 298 K, corresponding to an estimated molecular weight of 21 and 19 kDa, respectively. The molecular weight of the protein was also determined by mass-spectrometry analysis. The purified protein was first dialyzed against a low ionic strength solution (20 m*M* Tris–HCl pH 8.0, 100 m*M* NaCl) for 24 h. The sample was then run on a reverse-phase RP-C8 HPLC column (2.1 × 30 mm) using a gradient of 0–80%(*v*/*v*) acetonitrile in water before being introduced into an LCQ Classic mass spectrometer (Finnigan). Analysis of the purified hRheb GTPase domain showed a molecular weight of 20 008.0 Da, in agreement with the theoretical molecular weight of 20 123.1 Da calculated from the amino-acid sequence.

2.2. Crystallization

2.2.1. hRheb–GDP complex. The purified hRheb GTPase protein was first dialyzed against the storage buffer for 12 h and then concentrated to about 7 $mg\ ml^{-1}$ in an Amicon (Millipore) by centrifugation prior to crystallization. Crystallization was performed at 277 K using the hanging-drop vapour-diffusion method. Initial trials of crystallization conditions were carried out for the hRheb–GDP complex using screening kits from Hampton Research. Solution No. 42 of Crystal Screen I (50 m*M* KH_2PO_4 and 20% PEG 8000) produced small rod-shaped crystals (about 0.02 × 0.02 × 0.04 mm for the largest crystal). Optimization was performed by varying the PEG and salt concentration and the pH. Large single crystals (about 0.1 × 0.2 × 0.8 mm) of the hRheb–GDP complex were obtained by

Table 1
Summary of diffraction data statistics.

Values in parentheses refer to the highest resolution shell.

Complex	hRheb–GDP (form I)	hRheb–GDP (form I)	hRheb–GppNHp (form I)	hRheb–GppNHp (form II)	hRheb–GTP (form II)	hRheb–GTP (form III)
Substrate added	GDP	None	GppNHp	GppNHp	GTP	GTP
Resolution (Å)	14.8–2.5 (2.7–2.5)	19.8–2.5 (2.6–2.5)	19.8–2.8 (2.9–2.8)	12.0–2.8 (2.9–2.8)	15.0–2.8 (2.9–2.8)	19.9–2.8 (2.9–2.8)
Space group	$P2_12_12_1$	$P2_12_12_1$	$P2_12_12_1$	$C222_1$	$C222_1$	$P2_1$
Unit-cell parameters						
a (Å)	44.5	44.5	44.6	102.9	102.4	77.3
b (Å)	52.3	54.6	53.5	99.2	98.3	47.9
c (Å)	70.6	70.6	70.7	48.0	47.9	71.9
β (°)						89.0
Observed reflections	15260	25593	16879	16061	21293	35586
Unique reflections [$I > 0\sigma(I)$]	5784	5819	4342	6018	6145	11538
Completeness (%)	98.2 (100.0)	91.4 (91.5)	97.4 (100.0)	96.0 (100.0)	98.8 (98.5)	95.3 (95.3)
$R_{\rm merge}$†	0.020 (0.042)	0.112 (0.292)	0.080 (0.203)	0.158 (0.381)	0.156 (0.333)	0.116 (0.254)
Average $I/\sigma(I)$	28.0 (14.8)	5.6 (2.2)	7.5 (2.9)	5.1 (2.3)	3.9 (1.6)	5.5 (2.3)
Mosaicity	0.84	1.11	1.31	0.61	0.93	0.67
Molecules per AU	1	1	1	1	1	2
Solvent content (%)	40.1	42.6	41.5	59.8	59.2	63.0
$V_{\rm M}$ (Å^3 Da^{-1})	2.1	2.1	2.1	3.1	3.0	3.3

† $R_{\rm merge} = \sum_{hkl}\sum_i |I_i(hkl) - \langle I(hkl)\rangle| / \sum_{hkl}\sum_i I(hkl)$, where I_i is the observed intensity of the ith measurement of reflection hkl and $\langle I\rangle$ is the average intensity for multiple measurements.

streak-seeding using small crystals from a drop that consisted of equal volumes of protein solution (2 µl) containing 1 m*M* GDP and crystallization solution (2 µl) containing 50 m*M* KH_2PO_4 pH 4.6, 15–20% PEG 8000 equilibrated against 0.5 ml of the crystallization solution.

2.2.2. Apo-form hRheb. Attempts were made to crystallize apo-form hRheb from similar crystallization conditions to those used for the hRheb–GDP complex. 2 µl concentrated protein solution (7 mg ml^{-1}) was mixed with 2 µl crystallization solution (50 m*M* KH_2PO_4, 20% PEG 8000) to form a hanging drop that was equilibrated against 0.5 ml crystallization solution. No nucleotide substrate was added to either the protein solution or the crystallization solution. Streak-seeding with microcrystals of the hRheb–GDP complex was performed the next day and produced rod-shaped crystals within 2 d. The newly formed crystals were used to streak-seed fresh drops in subsequent crystallization. This process was repeated several times to ensure the removal of the hRheb–GDP complex from the original seeding and the growth of apo-form hRheb crystals.

2.2.3. hRheb–GppNHp complex. Crystals of hRheb in complex with the GTP analogue GppNHp were grown from a drop containing 2 µl protein solution, 0.5 µl 7 m*M* GppNHp and 2 µl crystallization solution (50 m*M* KH_2PO_4 pH 4.6, 15% PEG 8000) equilibrated against 0.5 ml crystallization solution. Microcrystals appeared the next day and did not grow larger. Those crystals were used for streak-seeding in subsequent crystallization experiments. Two different forms of crystals were grown from the same crystallization condition in about 3 d.

2.2.4. hRheb–GTP complex. Initial attempts to grow crystals of the hRheb–GTP complex were performed by streak-seeding, initially with the hRheb–GDP crystals and subsequently with newly formed crystals from a protein solution containing GTP (about a threefold excess of GTP over the protein) and the crystallization condition used for the hRheb–GDP complex. Those experiments produced crystals that have a similar morphology and unit-cell parameters to those of the hRheb–GDP complex. Later, these crystals were shown to be of the hRheb–GDP complex (see §3.4). In order to obtain crystals of the hRheb–GTP complex, the protein sample was specifically prepared using a method modified from that reported by Herrmann *et al.* (1996) prior to setting up crystallization. 5 ml of the purified protein (1.2 mg ml^{-1}) was exchanged into a buffer containing 20 m*M* Tris–HCl pH 8.0, 200 m*M* NaCl, 2 m*M* DTT, 0.02% NaN_3, 5 m*M* EDTA in an Amicon ultrafiltration tube (Pharmacia) and then concentrated to 1 ml. The concentrated protein was mixed with 1 ml 50 m*M* GTP (about a 150-fold excess of GTP over the protein) and then incubated at 277 K for 3 h. The mixture was finally loaded onto a 5 ml Superdex G-25 Desalting column (Pharmacia) pre-equilibrated with the storage buffer to remove the excess GTP substrate. The eluted protein from the G-25 column was subsequently concentrated to about 6 mg ml^{-1} in an Amicon (Millipore) by centrifugation prior to crystallization. Screening for crystallization conditions of the hRheb–GTP complex was carried out using sparse-matrix kits from Hampton Research (Crystal Screens I and II). Solution No. 37 (0.1 *M* sodium acetate pH 4.6, 8% PEG 4000) of Crystal Screen I produced large plate-shaped crystals (about 0.2 × 0.2 × 0.04 mm) and solution No. 3 (0.4 *M* $NH_4H_2PO_4$) of Crystal Screen I produced small thin plate-shaped crystals (about 0.1 × 0.1 × 0.02 mm).

2.3. Diffraction data collection

Preliminary diffraction characterization and diffraction data collection were performed using an in-house Rigaku R-AXIS IV^{++} image-plate detector and Cu $K\alpha$ radiation (wavelength of 1.5418 Å) generated with a Rigaku rotating-anode generator (50 kV and 100 mA) and focused with a confocal mirror. X-ray diffraction data were collected from crystals that were mounted with a nylon loop and flash-cooled in a cold gaseous stream of N_2 (100 K) following a quick dip in a cryoprotectant solution containing the crystallization solution and 12% PEG 400 or 20% glycerol. The oscillation was 0.5–1° and the exposure time was about 2–4 min. The diffraction data were recorded on dual image plates and processed and scaled together using *CrystalClear* (MSC; Pflugrath, 1999).

2.4. Preliminary structure analysis

Preliminary structure analysis was carried out to determine whether a nucleotide substrate was bound at the active site, what kind of substrate was bound at the active site and to guide further crystallization experiments. The hRheb structures were determined using the molecular-replacement (MR) method as implemented in *CNS* (Brünger *et al.*, 1998). A homologue model of the hRheb GTPase domain generated by the Swiss-Model server using the structures of the two most homologous small GTPases,

human Rap2A (PDB code 1kao; Cherfils *et al.*, 1997) and human Rap1A (PDB code 1gua; Nassar *et al.*, 1996), was used as the template model for MR search.

3. Results and discussion

Rheb is a small GTPase that has been shown to play an important role in the insulin-signalling pathway, mediating the repression process of the growth-factor-dependent and nutrient-dependent activation of the mTOR signalling by TSC1/2 complex. In order to gain insight into the biological functions of Rheb, we are performing structural and functional studies on the GTPase domain of human Rheb. The GTPase domain of hRheb (residues 1–169 fused with a His tag at the C-terminus) was expressed in *E. coli* and purified to homogeneity using a combination of Ni–NTA affinity chromatography and gel filtration. Dynamic light-scattering analysis indicated that the protein is homogeneously dispersed and forms a monomer in solution. We have cocrystallized the GTPase domain of hRheb in complexes with substrates GDP, GTP and the GTP analogue GppNHp using the hanging-drop vapour-diffusion method and carried out X-ray diffraction data collection and preliminary structural analyses of these complexes. A summary of the diffraction data statistics is given in Table 1.

3.1. hRheb–GDP complex

Large single crystals of the hRheb–GDP complex appeared in 2–3 d after streak-seeding and grew to approximate dimensions of 0.1 × 0.2 × 0.8 mm with a rod shape within a week (Fig. 1*a*). These crystals diffracted X-rays to better than 2.5 Å resolution and showed no significant decay upon X-ray exposure. A diffraction data set was collected to 2.5 Å resolution (Table 1). Preliminary diffraction data analyses by autoindexing and examination of systematic absences in the reduced data indicate that the crystals belong to the orthorhombic space group $P2_12_12_1$, with unit-cell parameters $a = 44.5$, $b = 52.3$, $c = 70.6$ Å (form I). There is one hRheb–GDP complex per asymmetric unit, corresponding to a Matthews coefficient (V_M) of 2.1 Å^3 Da^{-1} (Matthews, 1968) and an estimated solvent content of 40.1%. Preliminary structure determination of the Rheb–GDP complex using the MR method has revealed well defined electron density for the bound GDP substrate at the nucleotide-binding site and structure refinement is ongoing.

3.2. Apo-form hRheb

Attempts to crystallize the apo-form hRheb GTPase from similar crystallization conditions as the hRheb–GDP complex but without the addition of any substrate produced crystals in 2–3 d. These crystals have a similar morphology to those of the hRheb–GDP complex (Fig. 1*b*). A diffraction data set was collected to 2.5 Å resolution for these crystals (Table 1). Analysis of the diffraction data indicates that these crystals have the same unit-cell parameters and belong to the same space group as those of the hRheb–GDP complex (form I). Preliminary structural analysis indicates that these crystals are actually the hRheb–GDP complex and that there is a GDP molecule bound at the nucleotide-binding site. These results suggest that GDP has tight binding affinity with the hRheb GTPase and that the bound GDP must be copurified with the protein from the expression system, as no GDP was added in the crystallization solution.

3.3. hRheb-GppNHp complex

The hRheb–GppNHp complex has been crystallized in two crystal forms by streak-seeding using the same crystallization conditions as for the hRheb–GDP complex. One type of crystals has the same morphology as those of the hRheb–GDP complex and grew to typical dimensions of 0.1 × 0.2 × 0.8 mm in 3–5 d (Fig. 1*c*). A diffraction data set was collected to 2.80 Å resolution (Table 1). These crystals have the same unit-cell parameters and belong to the same space group as those of the hRheb–GDP complex (form I). The other type of crystals have a thin plate shape and grew to typical dimensions of 0.2 × 0.2 × 0.02 mm in about 3 d (Fig. 1*d*). The space group of these crystals was determined to be the orthorhombic $C222_1$, with unit-cell parameters $a = 102.9$, $b = 99.2$, $c = 48.0$ Å (form II). There is one hRheb–GppNHp complex per asymmetric unit, with a V_M value of 3.1 Å^3 Da^{-1} and a solvent content of 59.8%. These crystals diffract X-rays to better than 2.8 Å resolution and a diffraction data set has been collected (Table 1). Preliminary structure determinations of both crystal forms have confirmed the presence of GppNHp in the substrate-binding site.

3.4. hRheb–GTP complex

Initial attempts to grow crystals of the hRheb–GTP complex from the same crystallization conditions as the hRheb–GDP complex in the presence of an excess amount of GTP in the protein solution produced crystals that have similar morphology and unit-cell parameters to those of the hRheb–GDP complex. 2.8 Å resolution diffraction data were collected for those crystals. However, preliminary structure analysis indicated that the structure contains GDP at the substrate-binding site, suggesting that the hRheb GTPase domain may have an intrinsic GTPase activity that can hydrolyze GTP into GDP and/or that GDP has a much tighter binding affinity than GTP and the concentration of GTP was not sufficient to replace GDP at the nucleotide-binding site.

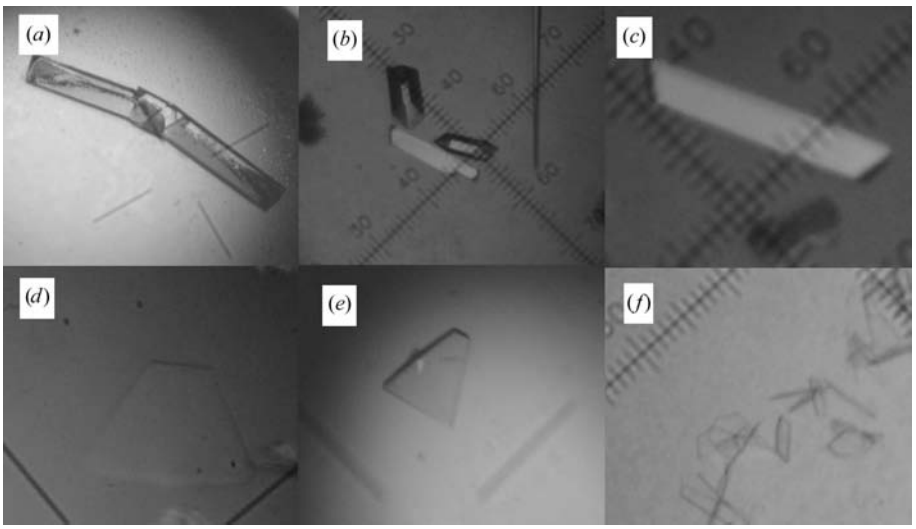

Figure 1
(*a*) Rod-shaped crystals of the hRheb–GDP complex in the presence of GDP (form I). (*b*) Rod-shaped crystals of the hRheb–GDP complex in the absence of GDP (form I). (*c*) Rod-shaped crystals of the hRheb–GppNHp complex (form I). (*d*) Plate-shaped crystals of the hRheb–GppNHp complex (form II). (*e*) Plate-shaped crystals of the hRheb–GTP complex (form II). (*f*) Small thin plate-shaped crystals of the hRheb–GTP complex (form III).

New crystallization screening of the hRheb–GTP complex yielded two different crystallization conditions that produced two types of crystals. One type of crystals had a thin plate shape similar to that of the form II type of crystals of the hRheb–GppNHp complex and grew to typical dimensions of $0.2 \times 0.2 \times 0.04$ mm in 3–5 d (Fig. 1*e*). They belong to space group $C222_1$, with unit-cell parameters $a = 102.4$, $b = 98.3$, $c = 47.9$ Å (form II) and a 2.80 Å resolution diffraction data set was collected (Table 1). The other type of crystals has small thin plate shape and grew to typical dimensions of $0.1 \times 0.1 \times 0.02$ mm in about 3 d (Fig. 1*f*). They belong to the monoclinic space group $P2_1$, with unit-cell parameters $a = 77.3$, $b = 47.9$, $c = 71.9$ Å, $\beta = 89.0^\circ$ (form III), and contain two hRheb–GTP complex per asymmetric unit, with a V_M value of 3.3 Å^3 Da^{-1} and a solvent content of 63.0%. A diffraction data set has been collected to 2.8 Å resolution (Table 1). Analysis of the lattice packing indicates that form III appears to be a non-isomorphic subgroup of form II. Preliminary structure determinations of both crystal forms have confirmed the presence of GTP at the substrate-binding site and further structure refinement is under way.

This study was supported in part by National Natural Science Foundation of China (NSFC) grants (30125011, 30170223 and 30130080), 863 Hi-Tech Program grants (2002BA711A13 and 2004AA235091) and Chinese Academy of Sciences grant (KSCX1-SW-17).

References

Brünger, A. T., Adams, P. D., Clore, G. M., DeLano, W. L., Gros, P., Grosse-Kunstleve, R. W., Jiang, J.-S., Kuszewski, J., Nilges, M., Pannu, N. S., Read, R. J., Rice, L. M., Simonson, T. & Warren, G. L. (1998). *Acta Cryst.* D**54**, 905–921.

Castro, A. F., Rebhun, J. F., Clark, G. J. & Quilliam, L. A. (2003). *J. Biol. Chem.* **278**, 32493–32496.

Cherfils, J., Menetrey, J., Le Bras, G., Janoueix-Lerosey, I., de Gunzburg, J., Garel, J. R. & Auzat, I. (1997). *EMBO J.* **16**, 5582–5591.

Clark, G. J., Kinch, M. S., Rogers-Graham, K., Sebti, S. M., Hamilton, A. D. & Der, C. J. (1997). *J. Biol. Chem.* **272**, 10608–10615.

Dabora, S. L., Jozwiak, S., Franz, D. N., Roberts, P. S., Nieto, A., Chung, J., Choy, Y. S., Reeve, M. P., Thiele, E., Egelhoff, J. C., Kasprzyk-Obara, J., Domanska-Pakiela, D. & Kwiatkowski, D. J. (2001). *Am. J. Hum. Genet.* **68**, 64–80.

Gao, X., Zhang, Y., Arrazola, P., Hino, O., Kobayashi, T., Yeung, R. S., Ru, B. & Pan, D. (2002). *Nature Cell Biol.* **4**, 699–704.

Garami, A., Zwartkruis, F. J., Nobukuni, T., Joaquin, M., Roccio, M., Stocker, H., Kozma, S. C., Hafen, E., Bos, J. L. & Thomas, G. (2003). *Mol. Cell*, **11**, 1457–1466.

Gingras, A. C., Raught, B. & Sonenberg, N. (2001). *Gene Dev.* **15**, 807–826.

Gomez, M. R. (1999). *Tuberous Sclerosis*, 3rd ed. Oxford University Press.

Gromov, P. S., Madsen, P., Tomerup, N. & Celis, J. E. (1995). *FEBS Lett.* **377**, 221–226.

Hentges, K. E., Sirry, B., Gingeras, A. C., Sarbassov, D., Sonenberg, N., Sabatini, D. & Peterson, A. S. (2001). *Proc. Natl Acad. Sci. USA*, **98**, 13796–13781.

Herrmann, C. (2003). *Curr. Opin. Struct. Biol.* **13**, 122–129.

Herrmann, C., Horn, G., Spaargaren, M. & Wittinghofer, A. (1996). *J. Biol. Chem.* **271**, 6794–6800.

Inoki, K., Li, Y., Xu, T. & Guan, K. L. (2003). *Genes Dev.* **17**, 1829–1834.

Inoki, K., Li, Y., Zhu, T., Wu, J. & Guan, K. L. (2002). *Nature Cell Biol.* **4**, 648–657.

Jaeschke, A., Hartkamp, J., Saitoh, M., Roworth, W., Nobukuni, T., Hodges, A., Sampson, J., Thomas, G. & Lamb, R. (2002). *J. Cell Biol.* **159**, 217–224.

Keith, C. T. & Schreiber, S. L. (1995). *Science*, **270**, 50–51.

Li, Y., Corradetti, M. N., Inoki, K. & Guan, K. L. (2004). *Trends Biochem. Sci.* **29**, 32–38.

Maheshwar, M. M., Cheadle, J. P., Jones, A. C., Myring, J., Fryer, A. E., Harris, P. C. & Sampson, J. R. (1997). *Hum. Mol. Genet.* **6**, 1991–1996.

Manning, B. D. & Cantley, L. C. (2003). *Trends Biochem. Sci.* **28**, 573–576.

Manning, B. D., Tee, A. R., Logsdon, M. N., Blenis, J. & Cantley, L. C. (2002). *Mol. Cell*, **10**, 151–162.

Matthews, B. W. (1968). *J. Mol. Biol.* **33**, 491–497.

Mizuki, N., Kimura, M., Ohno, S., Miyata, S., Sato, M., Ando, H., Ishihara, M., Goto, K., Watanabe, S., Yamazaki, M., Ono, A., Taguchi, S., Okumura, K., Nogami, M., Taguchi, T., Ando. A. & Inoko, H. (1996). *Genomics*, **34**, 114–118.

Montagne, J., Radimerski, T. & Thomas, G. (2001). *Sci. STKE*, **105**, PE36.

Nassar, N., Horn, G., Herrmann, C., Block, C., Janknecht, R. & Wittinghofer, A. (1996). *Nature Struct. Biol.* **3**, 723–729.

Paduch, M., Jelen, F. & Otlewski, J. (2001). *Acta Biochim. Pol.* **48**, 829–850.

Pan, D., Dong, J., Zhang, Y. & Gao, X. (2004). *Trends Cell Biol.* **14**, 78–85.

Pflugrath, J. W. (1999). *Acta Cryst.* D**55**, 1718–1725.

Povey, S., Burley, M. W., Attwood, J., Benham, F., Hunt, D., Jeremiah, S. J., Franklin, D., Gillett, G., Malas, S., Robson, E. B., Tippett, P., Edwards, J. H., Kwiatkowski, D. J., Super, M., Mueller, R., Fryer, A., Clarke, A., Webb, D. & Osborne, J. (1994). *Ann. Hum. Genet.* **58**, 107–127.

Reuther, G. W. & Der, C. J. (2000). *Curr. Opin. Cell Biol.* **12**, 157–165.

Saucedo, L. J., Gao, X., Chiarelli, D. A., Li, L., Pan, D. & Edgar, B. A. (2003). *Nature Cell Biol.* **5**, 566–571.

Sparagana, S. P. & Roach, E. S. (2000). *Curr. Opin. Neurol.* **13**, 115–119.

Stocker, H., Radimerski, T., Schindelholz, B., Wittwer, F., Belawat, P., Daram, P., Breuer, S., Thomas, G. & Hafen, E. (2003). *Nature Cell Biol.* **5**, 559–565.

Tee, A. R., Fingar, D. C., Manning, B. D., Kwiatkowski, D. J., Cantley, L. C. & Blenis, J. (2002). *Proc. Natl Acad. Sci. USA*, **99**, 13571–13576.

Tee, A. R., Manning, B. D., Roux, P. P., Cantley, L. C. & Blenis, J. (2003). *Curr. Biol.* **13**, 1259–1268.

Vetter, I. R. & Wittinghofer, A. (2001). *Science*, **294**, 1299–1304.

Yamagata, K., Sanders, L. K., Kaufmann, W. E., Yee, W., Barnes, C. A., Nathans, D. & Worley, P. F. (1994). *J. Biol. Chem.* **269**, 16333–16339.

Zhang, Q. H. *et al.* (2000). *Genome Res.* **10**, 1546–1560.

Zhang, Y., Gao, X., Saucedo, L. J., Ru, B., Edgar, B. A. & Pan, D. (2003). *Nature Cell Biol.* **5**, 578–581.